

## Short Notes

# Characterization of a Continuous, Very Narrowband Seismic Signal near 2.08 Hz

by Kelly H. Liu and Stephen S. Gao

**Abstract** We have detected a continuous seismic signal near 2.08 Hz using data from a portable seismic array, 1280 km long, deployed in Siberia and Mongolia. The signal can be observed on almost all the stations along the profile. The amplitude and the frequency of the signal show a clear daily cycle, and their temporal variations are similar at different stations, suggesting that the signals observed at different stations have a common source. We performed a nonlinear inversion of the amplitude of the signal and found that the geometrical-spreading factor is about 0.6, implying that the signal is most likely to be a form of surface waves. The source location found by the inversion is in the vicinity of the city of Irkutsk, which is about 50 km north of Lake Baikal.

### Introduction

The existence of very narrowband seismic signals, sometimes called spectral lines or monochromatic signals, has been known for a long time (Frantti, 1963; Plesinger and Wielandt, 1974; Hjortenberget and Risbo, 1975; Bokelmann and Baisch, 1999). The one that was studied most extensively has a peak at about 2.08 Hz and was generally considered to be generated by power networks in Europe and Asia, which have a frequency of 50 Hz. Previous studies found that the temporal variations in the frequency are usually very small, about 0.003 Hz or less and are irregular. On the other hand, the amplitudes vary significantly with time and space. In Norway's large seismic array station, NOR-SAR, area, Hjortenberget and Risbo (1975) found several monochromatic components, including 2.08, 2.78, 5.00, and 5.56 Hz. The conclusion from the study is that the 2.78-Hz signal was generated by a nearby hydroelectric power plant which runs its turbines at 166  $\frac{2}{3}$  revolutions per minute ( $166.66667/60 = 2.77778$ ). The 2.08-Hz signal was found to vary significantly in both time and space, and its source was not found. A recent study using data from the German Experimental Seismic System detected a clear signal at 2.08 Hz and was able to suggest that its source was located near the German-Czech border, although the physical device or devices that generated the signal were not identified. The same study found that the signal propagates to a distance of more than 300 km, possibly as a regional phase of *Lg* and/or *Sg* type with an apparent velocity of about 4 km/sec (Bokelmann and Baisch, 1999). It seems that at this moment, the physical device or devices that generated the 2.08-Hz signal have not been identified, mostly because of the lack of dense seismic network in the vicinity of the source.

### Data

In the summer of 1992, researchers from the University of California at Los Angeles, University of Wisconsin at Madison, and the Institute of the Earth's Crust of the Russian Academy of Sciences conducted a joint seismic experiment along a 1280-km-long profile traversing southern Siberia and north Mongolia (Fig. 1). Most of the seismographs that we used were RefTeks, which were programmed to record continuously at the rate of 10 samples/sec. Several stations were equipped with other types of seismographs. Short-period sensors (L4C, H10, and S13) with peak frequencies of 0.5–2 Hz and several broadband (STS-2, Guralp) seismometers were used. Results presented here were obtained using data from the short-period seismometers. About 5% of the data were used to study the velocity and attenuation structures and anisotropy of the upper mantle beneath the network (Gao *et al.*, 1994a,b, 1997). The majority of the data set without clear seismic arrivals shows a remarkable very narrowband signal.

### Temporal Variations of Amplitude and Frequency

In most of the stations, the signal is too weak to be observed on the seismograms directly. It is seen most clearly on the spectra. Figure 2 shows seismograms and their spectra for stations 9 and 10, which are 31.56 km apart (Fig. 1). The spectra of the noise sections before the arrival of a teleseismic event show an outstanding peak at about 2.08 Hz in both the stations. The signal can be observed in most of the stations along the profile, which extends to 1280 km from

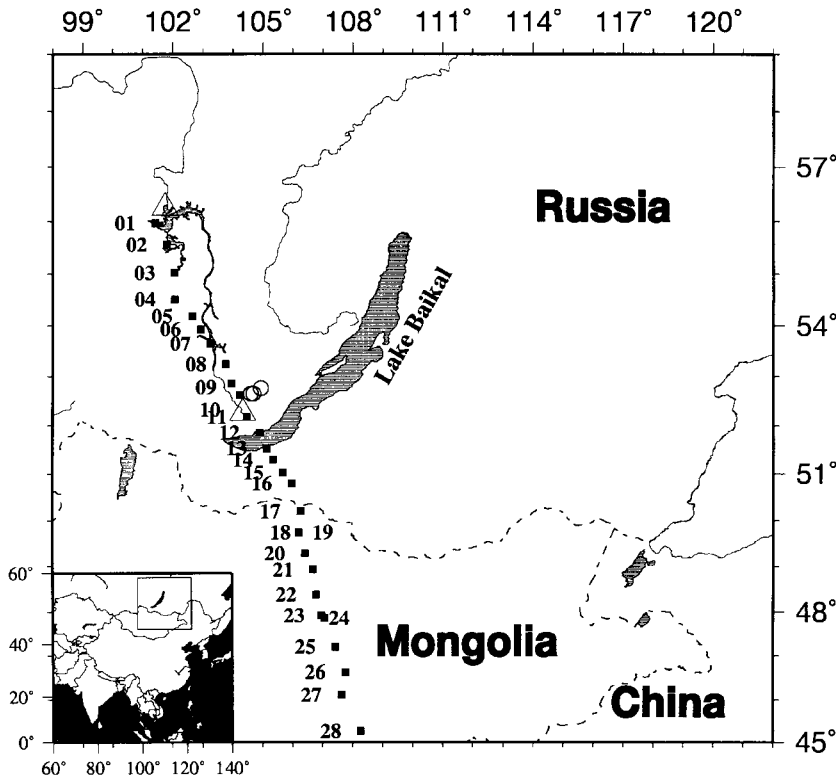


Figure 1. A Mercator projection map showing locations of stations used in the study. The two open triangles represent large hydroelectric power stations. The southern one is located in the city of Irkutsk, and the northern one is located at the north end of the profile.

north of Lake Baikal to southern Mongolia (Fig. 3). The signal can also be observed on GSN station TLY (Fig. 4) which is located near the SW tip of Lake Baikal.

For each station and each component, we search for  $A_m$ , the maximum amplitude on the spectrum in the frequency band of 2.05–2.15 Hz, and  $F_m$ , the frequency corresponding to  $A_m$ , using a series of 30-min time windows. Figures 5 and 6 show temporal variations of  $A_m$  for stations 9 and 10 for a 45-day time period. The most outstanding feature of Figures 5 and 6 is the remarkable similarity between data from the two stations. Between 92:229 and 92:237, the amplitude reduced to about 1/4 of the normal level. Similar variations can be observed in most of the other stations, although the signal-to-noise ratio is lower. The similarity at different stations suggests that the signals observed at different stations have a common source. The amplitudes seem to show a daily periodicity with the lowest values occurring at midnight coordinated universal time, which is 9 a.m. local time.

Figures 7 and 8 show the temporal variation of  $F_m$ , the frequency corresponding to the maximum amplitude in the frequency band of 2.05–2.15 Hz. The glitches are caused by earthquakes. The daily periodicity of the temporal variation of  $F_m$  is clear. Figure 9 suggests that  $A_m$  and  $F_m$  are negatively and significantly correlated, as indicated by the slopes and their standard deviations of the fitted lines.

#### Spatial Variation of Amplitude

We next estimate the mean Fourier amplitude at each station over a period of 35 hr from hr 1, day 204 to hr 11,

day 205. During the time period, no earthquakes with significant arrivals were recorded by the network. Fast Fourier transforms are performed for time windows of 1638.4 sec moving at an interval of 10 sec at each step.

For each time window, the peak amplitude in the frequency band of 2.05–2.15 Hz is taken as the total amplitude ( $A_m$ ); and the mean amplitude of background noise ( $A_n$ ) is calculated by averaging the amplitudes in the two frequency bands of (1.58, 1.88) Hz and (2.30, 2.60) Hz. The amplitude of the signal ( $A_s$ ) is then estimated using  $A_s = A_m - A_n$ .

The mean amplitude for a station is then estimated using  $A = 1/n \sum_{i=1}^n A_{si}$  where  $n$  is the number of time windows. To ensure high signal-to-noise ratio in the final results,  $A_s$  from a time window is not used in the averaging if  $A_m/A_n < 3.0$ . Figure 10 shows spatial variations of  $A$  along the profile. It is clear that stations 9 and 10 are located closest to the source of the signal. The signal can be seen in southern Mongolia, near the northern boundary of the Gobi desert, although the amplitude is about 0.1% of those at stations 9 and 10.

To further investigate the characteristics of the signal, we invert for its location and amplitude, the geometrical-spreading factor, and the product of the attenuation factor and propagating velocity by fitting the data shown in Figure 10 using

$$\ln(A_i) = \ln(A_0) - \alpha \ln(r_i) - \pi f \frac{r_i}{vQ} \quad (1)$$

where  $A_i$  is the amplitude of the signal at station  $i$ ;  $A_0$  is the amplitude of the signal at the source;  $r_i$  is the distance from

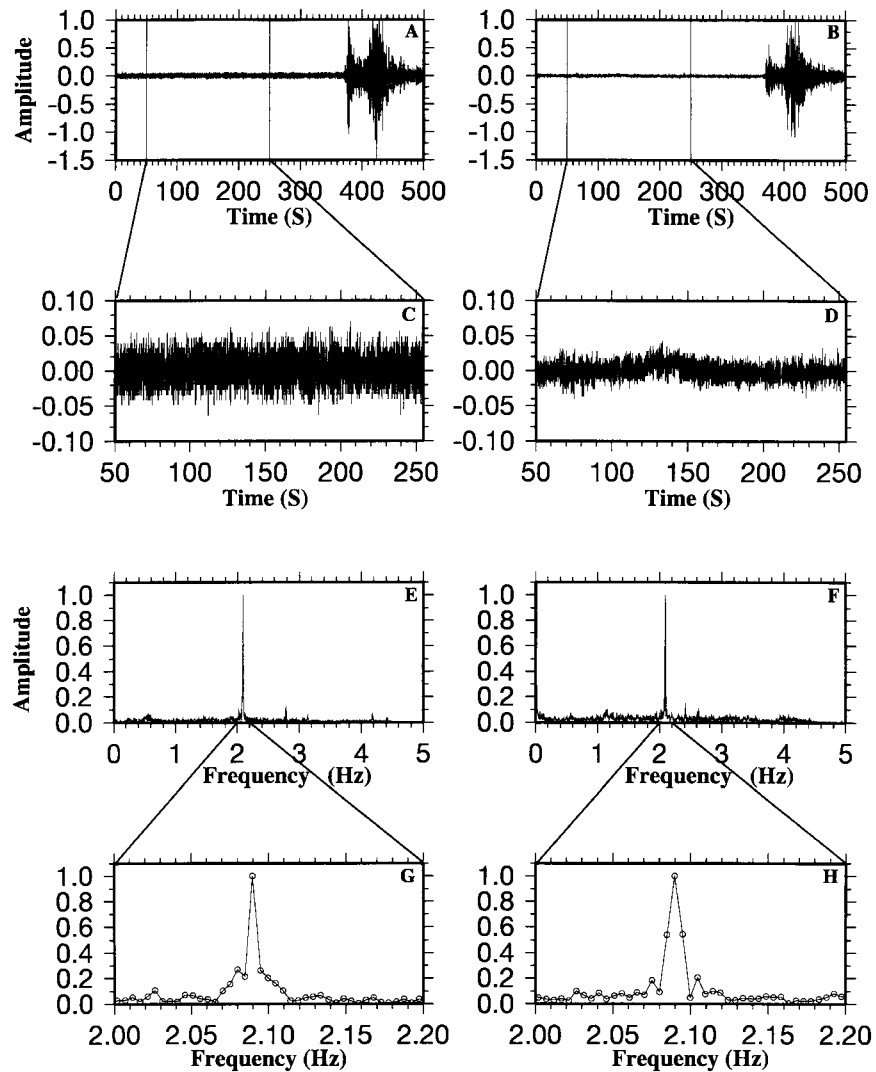


Figure 2. Seismograms and spectra of stations 9 (left) and 10 (right) for a 500-sec section starting from 92:205 07:00, recorded by the vertical component. The two stations are 31.56 km apart. (A) and (B) are recordings of a teleseismic event at the two stations. Both traces were normalized by their maximum amplitude; (C) and (D) are enlargements of the part between 50 and 250 sec in (A) and (B) where there are no clear earthquake wave arrivals; (E) and (F) are spectra of the data shown in (C) and (D); (G) and (H) are enlargements of (E) and (F) in the 2.0–2.2-Hz range. The spectra were normalized by the maximum amplitudes.

the source to station  $i$ , that is,  $r_i = \sqrt{(x_i - x_0)^2 + (y_i - y_0)^2}$ ;  $x_i$  is the E–W distance of the station from the origin;  $x_0$  the E–W distance of the source from the origin;  $y_i$  the N–S distance of the station from the origin;  $y_0$  the N–S distance of the source from the origin;  $f$  the frequency (2.08 Hz);  $\alpha$  the geometrical-spreading factor;  $v$  the propagating velocity, and  $Q$  the quality factor. A Bayesian inversion procedure (Jackson and Matsu'ura, 1985) is used for the inversion. In equation (1) the parameters to be found are  $A_0$ ,  $x_0$ ,  $y_0$ ,  $\alpha$ , and  $vQ$ . Note that  $v$  and  $Q$  cannot be separated for a monochromatic signal. Amplitudes on the vertical, N–S, and E–W components are used independently to obtain three groups of results (Table 1).

The results from the three components are similar to each other. The best-fitting geometrical-spreading factors are 0.69, 0.55, and 0.49 for the vertical, N–S, and E–W components, respectively, implying that the signal is most likely to be in the surface wave category, most likely as its multiply-reflected form such as  $Lg$  or  $Sg$ . The best-fitting  $vQ$  values were found to be about 1700 km/sec. If we use the typical propagating velocity of 3.5 km/sec for  $Lg$ , a  $Q$  of 485 is obtained, which is comparable to the crustal  $Q_s$  value predicted by the IASP91 Earth model (Kennett and Engdahl, 1991). The source locations of the signal found by using the vertical and the horizontal components are close to each other (Fig. 1).

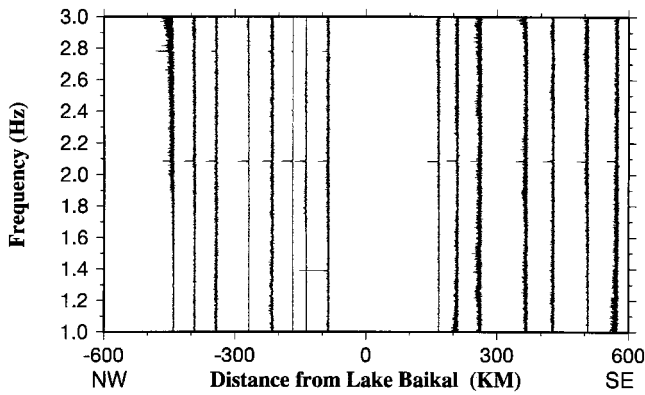


Figure 3. Fourier spectra for data recorded on day 225 plotted at the location of the recording stations relative to the center of Lake Baikal. The spectra were normalized by the maximum amplitude in the 1.5–2.5-Hz band.

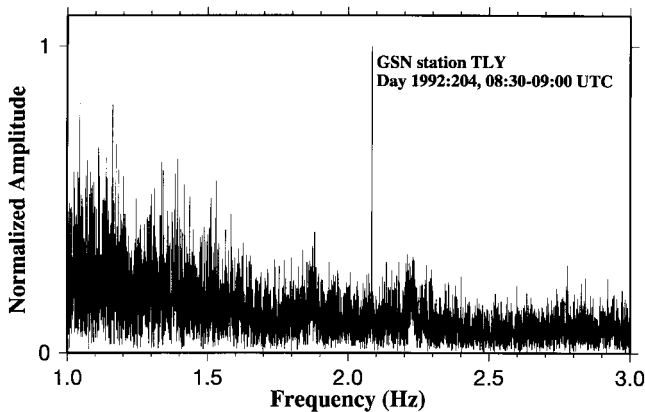


Figure 4. Fourier spectrum of a 30-min-long time series recorded by the vertical component of GSN station TLY starting at 92:204 08:30. The narrowband signal at 2.08 Hz is clearly observed.

### Discussion and Conclusions

A very narrowband seismic signal with frequency near 2.08 Hz is observed in Siberia and Mongolia. It is observable in most of the stations along a 1280-km seismic array. Similarity in temporal variations of the amplitudes at different stations suggests that the signals recorded at different stations have a common source. Such a perfect signal is most likely to be achieved by modern machinery. One of the possible sources is a hydroelectric power station in the city of Irkutsk (Fig. 1). The frequency of the electricity from the power station is 50 Hz, and there are 12 pole pairs on each rotor. The combination leads to a rotating frequency of  $50/24 = 2.08333$  Hz, or 125 revolutions/min. However, another power station, similar to the one at Irkutsk in terms of equipment and construction types but with several times larger energy output, is located near the northern end of the

profile (Fig. 1). Spatial variations of the amplitudes (Fig. 10) suggest that no significant 2.08 Hz signals are generated by this power station. This may be explained if rotors in different power plants show different degrees of asymmetry and thus different efficiencies in generating elastic waves in the subsurface. The daily variation in amplitude and frequency (Figs. 5–8) is hard to explain. One possibility is that it is caused by the daily variations in the loading of the electrical network. A decrease in the resistance to the rotors should lead to the decrease in the amplitude of the 2.08-Hz signal, and consequently to the increase of rotating frequency.

### Acknowledgments

The data set used in this study was recorded by a portable seismic network operated jointly by Institute of Earth's Crust of the Russian Academy of Sciences, University of Wisconsin, Madison, and University of California, Los Angeles. Special thanks are given to Yu. Zorin, N. Logatchev, V. Mordvinova, V. Kozhevnikov, P. Davis, and the late R. Meyer. Discussions with Paul Silver, Paul Davis, Leon Knopoff, and Goetz Bokelmann greatly improved the manuscript. This work was supported by DARPA under Contract F2901-91-K-DB17, and by NSF under Contracts EAR-0001000 and EPS-9874732.

### References

- Bokelmann, G. H. R., and S. Baisch (1999). Nature of narrowband signals at 2.083 Hz, *Bull. Seism. Soc. Am.* **89**, 156–164.
- Frantti, G. E. (1963). The nature of high frequency earth noise spectra, *Geophysics* **28**, 547–562.
- Gao, S., P. M. Davis, H. Liu, P. D. Slack, A. W. Rigor, Yu. A. Zorin, V. V. Mordvinova, V. M. Kozhevnikov, and N. A. Logatchev (1997). SKS splitting beneath continental rift zones, *J. Geophys. Res.* **102**, 22,781–22,797.
- Gao, S., P. M. Davis, H. Liu, P. Slack, Yu. A. Zorin, N. A. Logatchev, M. Kogan, P. Burkholder, and R. P. Meyer (1994a). Asymmetric up-warp of the asthenosphere beneath the Baikal rift zone, Siberia, *J. Geophys. Res.* **99**, 15,319–15,330.
- Gao, S., P. M. Davis, H. Liu, P. D. Slack, Yu. A. Zorin, V. V. Mordvinova, V. M. Kozhevnikov, P. D. Burkholder, and R. P. Meyer (1994b). Seismic anisotropy and mantle flow beneath the Baikal rift zone, *Nature* **371**, 149–151.
- Hjortenber, E., and T. Risbo (1975). Monochromatic components of the seismic noise in the NORSAR area, *R. Astron. Soc. Geophys. J.* **42**, 547–554.
- Jackson, D. D., and M. Matsu'ura (1985). A Bayesian approach to nonlinear inversion, *J. Geophys. Res.* **90**, 581–591.
- Kennett, B. L. N., and E. R. Engdahl (1991). Travel times for global earthquake location and phase identification, *Geophys. J. Int.* **105**, 429–465.
- Plesinger, A., and E. Wielandt (1974). Seismic noise at 2 Hz in Europe, *J. Geophys.* **40**, 131–136.

Department of Geology  
 Kansas State University  
 Manhattan, Kansas 66506  
 liu@ksu.edu

Manuscript received 17 March 2001.

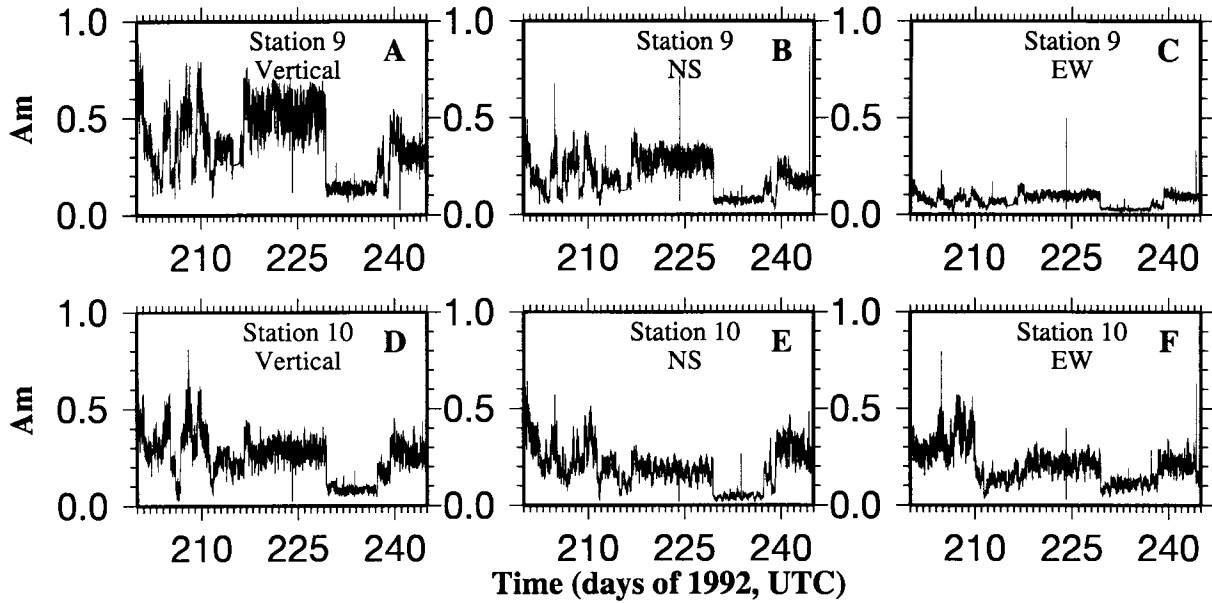


Figure 5. Temporal variations of the maximum Fourier amplitude,  $A_m$ , in the frequency band 2.05–2.15 Hz for station 9 (A–C) and 10 (D–F) during a 45-day period starting from day 200. (A) and (D), (B) and (E), and (C) and (F) are from the vertical, N-S, and E-W components, respectively. The traces were normalized by the maximum amplitude on the vertical component of station 9.

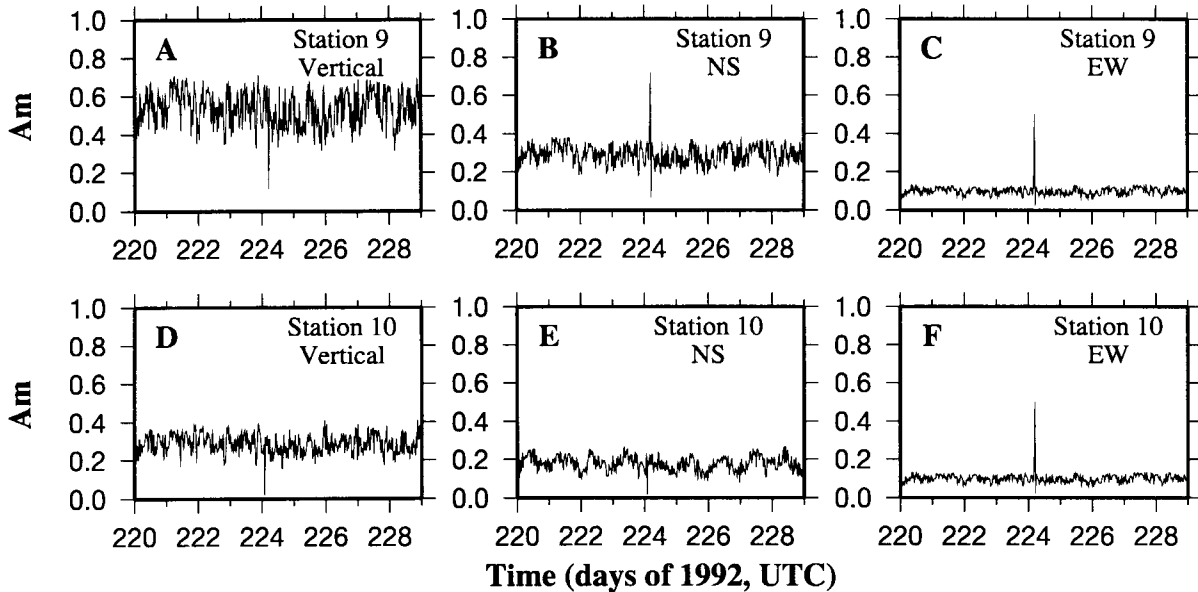


Figure 6. Same as Figure 5 but for a 9-day period from 92:220 to 92:229.

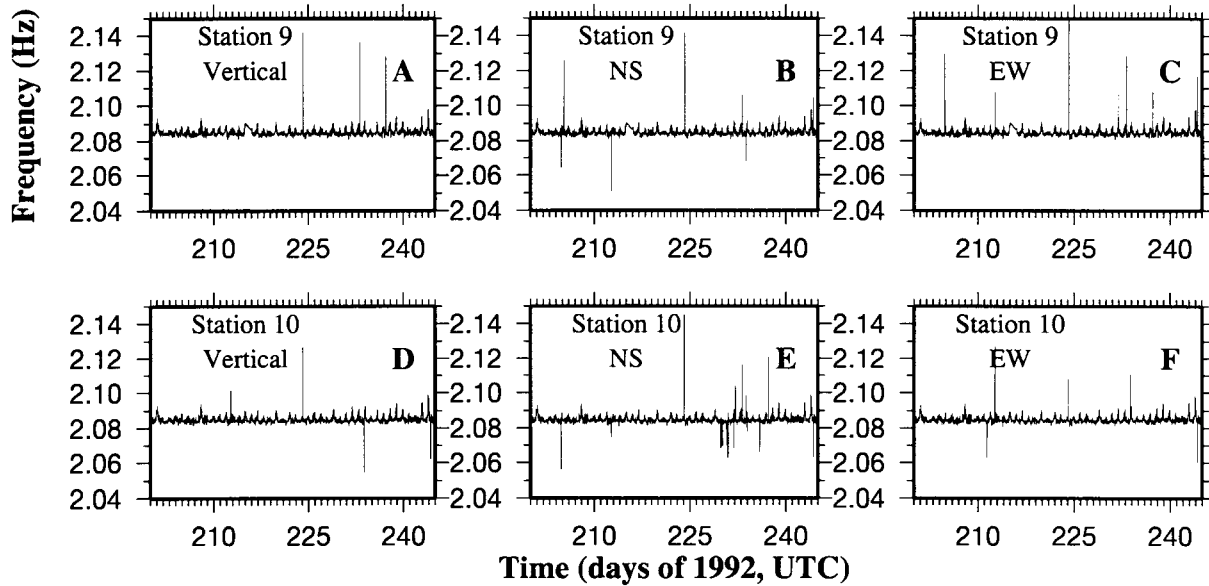


Figure 7. Temporal variations of  $F_m$ , the frequency corresponding to the maximum amplitude in the frequency band of 2.05–2.15 Hz, for stations 9 (A–C) and 10 (D–F). (A) and (D), (B) and (E), and (C) and (F) are from the vertical, N–S, and E–W components, respectively.

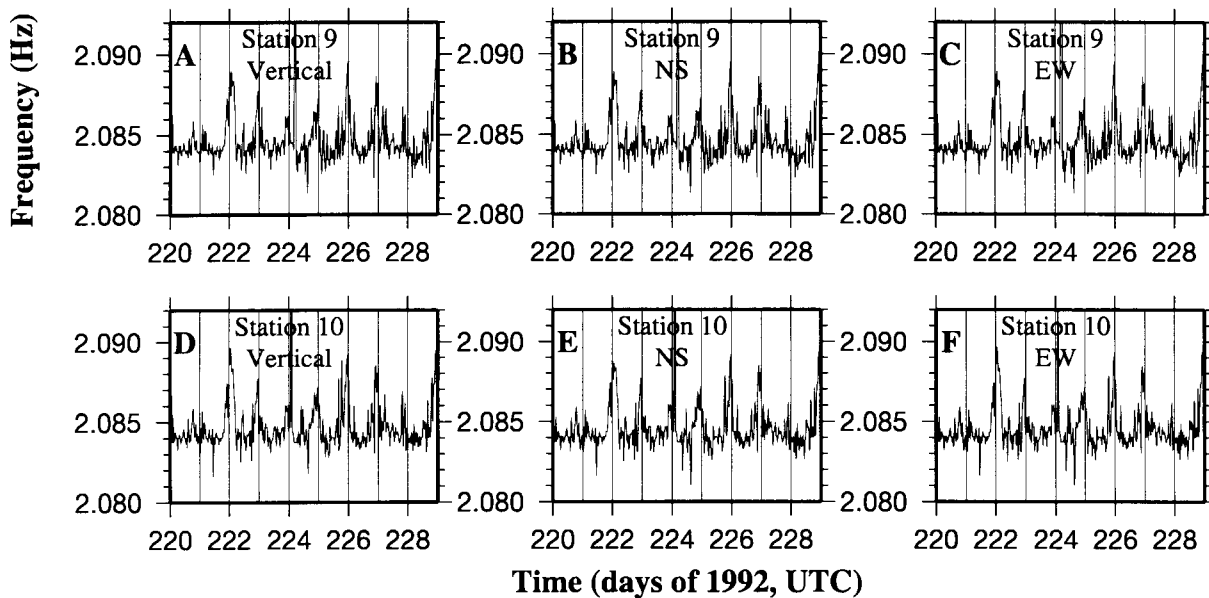


Figure 8. Same as Figure 7 but for the 9-day period from 92:220 to 92:229.

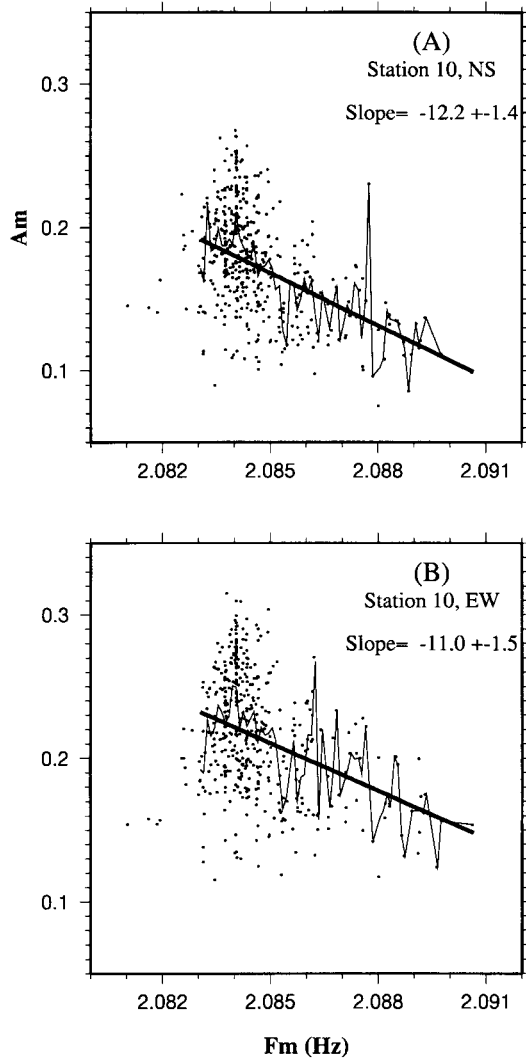


Figure 9. Plot of  $A_m$  against the corresponding  $F_m$  for the two horizontal components of station 10 for the period of 92:220–92:229. (A) N–S; (B) E–W. Dots represent the original data, thin lines represents mean values in successive frequency windows of 0.0001 Hz wide, and thick straight lines are the best-fitting results of the mean values.

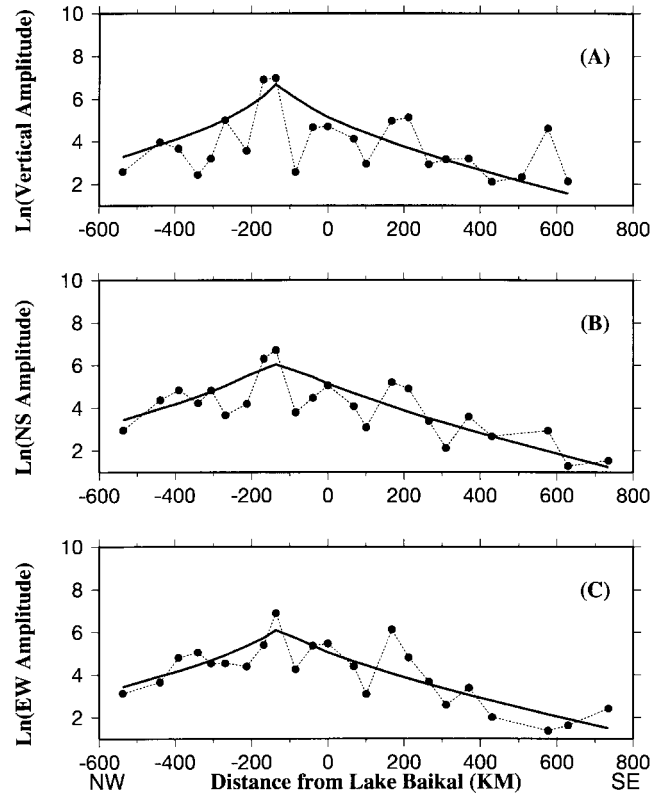


Figure 10. Observed (dotted) and fitted (solid) mean Fourier amplitudes during a 35-hr period starting at hr 1, day 204, for the (A) vertical, (B) N–S, and (C) E–W components. See equation (1) for the fitting function.

Table 1  
Results of Nonlinear Inversion

	Vertical	N–S	E–W	Explanations
$A_0$	9.00	8.39	7.89	Normalized amp.
$\alpha$	0.69	0.55	0.49	Spreading factor
$X_0$	104.60	104.94	104.69	Longitudes in degrees
$Y_0$	52.65	52.76	52.65	Latitudes in degrees
$vQ$	1725.73	1654.63	1820.19	Product of velocity and $Q$